ELSEVIER

Electrical Power and Energy Systems 22 (2000) 521–530

ELECTRICAL POWER & ENERGY SYSTEMS

www.elsevier.com/locate/ijepes

Convergence of the backward/forward sweep method for the load-flow analysis of radial distribution systems

E. Bompard, E. Carpaneto*, G. Chicco, R. Napoli

Dipartimento di Ingegneria Elettrica Industriale, Politecnico di Torino, Corso Duca degli Abruzzi 24, 10129 Turin, Italy

Abstract

This paper presents a study on the convergence characteristics of the backward/forward sweep method, which is one of the most effective methods for the load-flow analysis of the radial distribution systems. After revisiting the theoretical background, the convergence conditions and the evolution of the iterative process are investigated in detail for different load models. A dedicated study of the properties of the backward/forward sweep method is performed, taking into account different line X/R ratios and different types of voltage-dependent loads. Some useful indicators are introduced to estimate the number of iterations required to reach the convergence of the iterative process under a given tolerance. Test results are included for a tutorial two-node system and for a real 84-node system. © 2000 Elsevier Science Ltd. All rights reserved.

Keywords: Distribution systems; Radial networks; Load-flow; Load modelling

1. Introduction

The distribution systems are structurally weakly meshed but are typically operated with a radial structure. The computational methods proposed in the literature for the load-flow analysis of radial distribution systems adopt either the same algorithms used in the transmission systems analysis or dedicated methods which exploit the radial structure of the network. The computational methods can be grouped into two basic classes. The first class includes the direct methods, defined using only the basic circuit laws. The backward/forward sweep [1–3] and other methods based on the calculation of the node equivalents [4,5] belong to this class. The other class is composed of methods which require also information on the derivatives of the network equations. The traditional Newton–Raphson method and its modifications [6,7] belong to this class, as well as the Fast Decoupled Load Flow method [8] which is widely used for its efficiency in transmission system analysis but is quite less effective in the analysis of distribution systems with low line X/R ratios. Some specific methods suitable for the analysis of weakly meshed networks have also been proposed [1,9,10].

This paper analyses in detail the convergence of the backward/forward sweep method with different load models. The effectiveness of the backward/forward sweep method in the analysis of radial distribution systems has already been proven by comparing it to the traditional Gauss–Seidel and Newton–Raphson methods [11]. Section 2 of the paper is dedicated to the definition of the network structure. The formulation of the backward/forward sweep method is recalled in Section 3, where the iterative process if reformulated in a form suitable for the analysis of the convergence characteristics. Section 4 is dedicated to the formulation and discussion of the convergence conditions. Sections 5 and 6 illustrate the results of the numerical tests performed on a tutorial two-node system and on a real 84-node rural distribution system [5]. Section 7 summarises the conclusions.

2. Network structure and definitions

Let us consider a radial network with $n + 1$ nodes fed at constant voltage at the root node (node 0), as in Fig. 1. For each ith node, let us define $path(i)$ as the ordered list of the nodes encountered starting from the root (not included in the list) and moving to the ith node. Furthermore, each node belongs to a layer [12], which represents the position of the node in the network. For the ith node, $layer(i) = \text{dimension}(path(i))$. As an example, for node #7 in Fig. 1, $path(7) = \{1; 3; 7\}$and $layer(7) = 3$.

* Corresponding author. Tel.: + 39-011-564-7138; fax: + 39-011-564-7199.

E-mail address: carpaneto@polito.it (E. Carpaneto).

PII: S0142-0615(00)00009-0

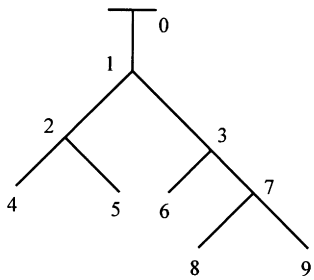

Fig. 1. Radial network structure.

The following criterion is assumed for node and line numbering:

- the nodes are numbered sequentially in ascending order proceeding from layer to layer (Fig. 1), in such a way that any path from the root node to a terminal node encounters nodes numbered in the ascending order;
- each branch starts from the sending bus (at the root side) and is identified by the number of its (unique) ending bus.

The above numbering leads to a particularly convenient system representation, in which both the node-to branch incidence matrix $\mathbf{L} \in N^{n,n}$ (root node not included) and its inverse $\boldsymbol{\Gamma} = \mathbf{L}^{-1} \in N^{n,n}$ are lower-triangular. Assuming for each branch a conventional value $+1$ for the sending bus and -1 for the ending bus, the generic component l_{ij} of the matrix $\mathbf{L}$ is

$$l_{ij} = \begin{cases} -1 & \text{if } i = j \\ 1 & \text{if } j = \text{sending bus (branch } i\text{)} \\ 0 & \text{otherwise} \end{cases}$$

while the generic component γ_{ij} of the matrix $\boldsymbol{\Gamma}$ is

$$\gamma_{ij} = \begin{cases} -1 & \text{if } j \in path(i) \\ 0 & \text{otherwise} \end{cases}$$

In the jth column of the matrix $\mathbf{L}$, the rows with non-zero terms correspond to the branches having the jth node as sending bus. In the jth column of the matrix $\boldsymbol{\Gamma}$, the rows with non-zero terms correspond to the nodes belonging to the branches derived from the jth node.

In the absence of mutual coupling between branches, it is possible to build the matrix $\boldsymbol{\Gamma}$ directly by visual inspection, without inverting the matrix $\mathbf{L}$. With a proper arrangement of the computational program, it is also possible to avoid the storage of the elements of the matrices $\mathbf{L}$ and $\boldsymbol{\Gamma}$.

For the system in Fig. 1, the two matrices are written as follows (zeros are omitted):

$$\mathbf{L} = \left|\begin{matrix} -1 & & & & & & & & \\ 1 & -1 & & & & & & & \\ 1 & & -1 & & & & & & \\ & 1 & & -1 & & & & & \\ & 1 & & & -1 & & & & \\ & & 1 & & & -1 & & & \\ & & 1 & & & & -1 & & \\ & & & & & & 1 & -1 & \\ & & & & & & 1 & & -1 \end{matrix}\right|$$

$$\boldsymbol{\Gamma} = \left|\begin{matrix} -1 & & & & & & & & \\ -1 & -1 & & & & & & & \\ -1 & & -1 & & & & & & \\ -1 & -1 & & -1 & & & & & \\ -1 & -1 & & & -1 & & & & \\ -1 & & -1 & & & -1 & & & \\ -1 & & -1 & & & & -1 & & \\ -1 & & -1 & & & & -1 & -1 & \\ -1 & & -1 & & & & -1 & & -1 \end{matrix}\right|$$

The distribution lines are modelled with the usual Π circuit. The electrical variables at every node (root excluded) and branches are represented by the following vectors:

$\mathbf{v} = [\underline{V}_1, \ldots, \underline{V}_i, \ldots, \underline{V}_n]^{\mathrm{T}}$, node voltages;
$\mathbf{i}_{\mathrm{B}} = [\underline{I}_{\mathrm{B}1}, \ldots, \underline{I}_{\mathrm{B}i}, \ldots, \underline{I}_{\mathrm{B}n}]^{\mathrm{T}}$, branch currents circulating in the series line impedance;
$\mathbf{i}_{\mathrm{L}} = [\underline{I}_{\mathrm{L}1}, \ldots, \underline{I}_{\mathrm{L}i}, \ldots, \underline{I}_{\mathrm{L}n}]^{\mathrm{T}}$, load currents;
$\mathbf{i}_{\mathrm{S}} = [\underline{I}_{\mathrm{S}1}, \ldots, \underline{I}_{\mathrm{S}i}, \ldots, \underline{I}_{\mathrm{S}n}]^{\mathrm{T}}$, total shunt currents, absorbed by shunt line admittances and loads;
$\mathbf{s}_{\mathrm{L}} = [\underline{S}_{\mathrm{L}1}, \ldots, \underline{S}_{\mathrm{L}i}, \ldots, \underline{S}_{\mathrm{L}n}]^{\mathrm{T}}$, complex load powers.

For the root node, let us define:

$\underline{V}_0$, root node voltage; assuming the angle of $\underline{V}_0$ as the angle reference for the system, $\underline{V}_0 = V_0 \mathbf{e}^{j0}$;
$\underline{I}_0$, net current injected in the root node;
$\underline{Y}_{\mathrm{S}0}$, total shunt admittance due to the shunt line parameters and to the equivalent admittance of the load connected to the root node.

For our purposes, it is also useful to define three diagonal matrices:

$\mathbf{Z}_{\mathrm{B}} \in C^{n,n}$ containing the series impedance of the branches;
$\mathbf{Y}_{\mathrm{B}} = \mathbf{Z}_{\mathrm{B}}^{-1} \in C^{n,n}$ containing the series admittance of the branches.
$\mathbf{Y}_{\mathrm{S}} \in C^{n,n}$ containing the total shunt admittance at each

node, due to the contribution of the shunt line parameters and of the equivalent load admittance. The equivalent load admittance depends on the load model, e.g. a load located at the ith node having a complex power $\underline{S}_{\mathrm{L}\,i}$ introduces in the matrix $\mathbf{Y}_{\mathrm{S}}$ an additive diagonal term $y_{\mathrm{S}i} = \underline{S}^*_{\mathrm{L}\,i}/V_i^2$.

3. The backward/forward sweep method

Let us consider a radial network with a unique generator which imposes the constant voltage V_0 in the root node. Starting from the initial node voltages $\mathbf{v}^{(0)} = [\underline{V}_1^{(0)},\dots,\underline{V}_n^{(0)}]^{\mathrm{T}}$, the backward/forward sweep method for the load-flow computation is an iterative method in which, at each iteration, two computational stages are performed:

1. *Backward stage:* the load currents $\mathbf{i}_{\mathrm{L}}^{(k)}$ and the subsequent shunt currents $\mathbf{i}_{\mathrm{S}}^{(k)} = f(\mathbf{v}^{(k-1)})$ are computed on the basis of the voltage vector $\mathbf{v}^{(k-1)}$ at the preceding iteration. Note that, in general, different voltage-dependent load representations are possible, as shown in the sequel. The resulting branch currents are given by

$$\mathbf{i}_{\mathrm{B}}^{(k)} = \mathbf{\Gamma}^{\mathrm{T}}\mathbf{i}_{\mathrm{S}}^{(k)} \tag{1}$$

2. *Forward stage:* the node voltages are updated on the basis of the voltage at the root node and of the voltage drops on the distribution lines evaluated by using the current $\mathbf{i}_{\mathrm{B}}^{(k)}$ computed in the backward stage, with

$$\mathbf{v}^{(k)} = -\mathbf{\Gamma}\mathbf{Z}_{\mathrm{B}}\mathbf{i}_{\mathrm{B}}^{(k)} + V_0\mathbf{l} \tag{2}$$

where $\mathbf{l} \in N^n$ is a vector composed of all unity terms. In the absence of shunt line parameters and loads, Eq. (2) has the trivial solution $\mathbf{v} = V_0\mathbf{l}$.

The backward/forward sweep method is now reformulated in a way suitable for the analysis of the convergence of the iterative process. Let us start from the system of equations

$$\begin{vmatrix} \underline{I}_0 \\ \mathbf{0} \end{vmatrix} = \begin{vmatrix} \underline{Y}_{S0} & \mathbf{y}_0^{\mathrm{T}} \\ \mathbf{y}_0 & \mathbf{Y}' \end{vmatrix} \begin{vmatrix} V_0 \\ \mathbf{v} \end{vmatrix} \tag{3}$$

where the vector $\mathbf{y}_0$ contains non-zero terms for the components corresponding to the nodes directly connected to the root and zero elsewhere, and the matrix $\mathbf{Y}' \in C^{n,n}$ has the following definition:

$$\mathbf{Y}' = \mathbf{L}^{\mathrm{T}}\mathbf{Y}_{\mathrm{B}}\mathbf{L} + \mathbf{Y}_{\mathrm{S}} \tag{4}$$

Rewriting the last n rows of Eq. (3) yields

$$(\mathbf{L}^{\mathrm{T}}\mathbf{Y}_{\mathrm{B}}\mathbf{L} + \mathbf{Y}_{\mathrm{S}})\mathbf{v} + \mathbf{y}_0 V_0 = \mathbf{0} \tag{5}$$

The iterative process is set up by rearranging Eq. (5) in the form $\mathbf{v}^{(k)} = f(\mathbf{v}^{(k-1)})$. Starting from the initial voltage vector $\mathbf{v}^{(0)}$, at the kth iteration:

$$\mathbf{v}^{(k)} = -\mathbf{\Gamma}\mathbf{Z}_{\mathrm{B}}\mathbf{\Gamma}^{\mathrm{T}}\mathbf{Y}_{\mathrm{S}}^{(k-1)}\mathbf{v}^{(k-1)} + V_0\mathbf{l} \tag{6}$$

The iterative process terminates when the maximum variation of the complex voltage at any node in two successive iterations is lower than a specified voltage tolerance ΔV_{MAX}. The above procedure is formally equivalent to the backward/forward sweep method with backward stage $\mathbf{i}_{\mathrm{B}}^{(k)} = \mathbf{\Gamma}^{\mathrm{T}}\mathbf{Y}_S^{(k-1)}\mathbf{v}^{(k-1)}$ and forward stage $\mathbf{v}^{(k)} = -\mathbf{\Gamma}\mathbf{Z}_{\mathrm{B}}\mathbf{i}_{\mathrm{B}}^{(k)} + V_0\mathbf{l}$.

4. Convergence of the iterative process

4.1. Convergence conditions

The convergence characteristics of the iterative process are analysed in this section, extending some results previously reported in the literature [13]. For $k \geq 1$, let us rewrite Eq. (6) in the form

$$\mathbf{v}^{(k)} = \mathbf{B}^{(k-1)}\mathbf{v}^{(k-1)} + \mathbf{v}^{(0)} \tag{7}$$

where

$$\mathbf{B}^{(k)} = -\mathbf{\Gamma}\mathbf{Z}_{\mathrm{B}}\mathbf{\Gamma}^{\mathrm{T}}\mathbf{Y}_{\mathrm{S}}^{(k)} \tag{8}$$

If all the loads have constant admittance, the matrix $\mathbf{B}$ is independent of k. In this case, considering a suitable norm (e.g. the unity norm $\|\mathbf{B}\|_1$ or the infinite norm $\|\mathbf{B}\|_\infty$ defined in the Appendix A), a sufficient condition for convergence is

$$\|\mathbf{B}\| < 1 \tag{9}$$

If there is at least one load with non-constant admittance, the condition (9) is not rigorously valid. Anyway, at low loading, the voltage variation is low and the effect of the voltage dependency is quite limited, as shown in the numerical examples presented in the following sections.

4.2. Upper bounds for the convergence conditions

In order to get some qualitative information on the convergence of the iterative process Eq. (7), a most restrictive sufficient condition is defined. Assuming all constant admittance loads, an upper bound is computed for the unity norm $\|\mathbf{B}_1\|$ using all the matrices involved in Eq. (8) and satisfying the inequalities

$$\|\mathbf{B}\|_1 < \|\mathbf{\Gamma}^{\mathrm{T}}\|_1\|\mathbf{Z}_{\mathrm{B}}\|_1\|\mathbf{\Gamma}\,\|_1\|\,\mathbf{Y}_{\mathrm{S}}\|_1 < 1 \tag{10}$$

Considering the terms in Eq. (10), it is possible to observe that:

- $\|\mathbf{\Gamma}\,\|_1^{\mathrm{T}}$ is the number n_{L} of network layers, which varies from $n_{\mathrm{L}} = 1$ (star topology) to $n_{\mathrm{L}} = n$ (unique feeder);
- $\|\mathbf{\Gamma}_1\|$ is the maximum number n_{V} of nodes located after any node of the system; $n_{\mathrm{V}} = n$ if the root node is connected to a unique node, otherwise it is possible to separate different subsystems, and n_{V} is the maximum number of nodes contained in a single subsystem;

- $\|\mathbf{Z}_{\mathrm{B}}\|_1$ is the maximum magnitude $Z_{\mathrm{B}}^{\mathrm{MAX}}$ of a single branch impedance;
- $\|\mathbf{Y}_{\mathrm{S}}\|_1$ is the maximum magnitude $Y_{\mathrm{S}}^{\mathrm{MAX}}$ of a shunt admittance (including loads and shunt line parameters).

The sufficient condition for convergence is then overestimated by assuming

$$n_{\mathrm{L}} n_{\mathrm{V}} Z_{\mathrm{B}}^{\mathrm{MAX}} Y_{\mathrm{S}}^{\mathrm{MAX}} < 1 \tag{11}$$

This inequality is useful to qualitatively explain how the convergence is affected by system structure and loading conditions. Let us consider an initial operating point, and let us introduce some change in the system. The solution point becomes closer to the convergence limit:

- for any load increase (corresponding to increase some element in the matrix $\mathbf{Y}_{\mathrm{S}}$);
- for any increase in the series impedance of a branch (i.e. increasing some elements in the matrix $\mathbf{Z}_{\mathrm{B}}$);
- after structural modifications (e.g. a system reconfiguration) which increase the number of the network layers or the number of nodes.

It is possible to obtain a less restrictive sufficient condition for convergence by writing

$$\|\mathbf{B}\|_1 < \|\boldsymbol{\Gamma}^{\mathrm{T}} \mathbf{Z}_{\mathrm{B}} \boldsymbol{\Gamma}\|_1 \|\mathbf{Y}_{\mathrm{S}}\|_1 < 1 \tag{12}$$

Using the terms defined in Eqs. (A2) and (A3) in the Appendix A, Eq. (12) may be written as

$$\max_{j=1,\dots,n} (Z_{\mathrm{U}j} Y_{\mathrm{S}jj}) < 1 \tag{13}$$

For a given network, it is possible to compute $Z_{\mathrm{U}j}$ for each jth column on the basis of network structure and series line impedance, without considering shunt parameters and loads. Then, for any load pattern, the sufficient conditions for the convergence of the iterative process will depend on the type of load. If all the loads have constant admittance, Eq. (13) directly gives a set of limit admittance values. The convergence limit is reached if the system is simultaneously charged in each jth node with the corresponding limit admittance $1/Z_{\mathrm{U}_j}$. Nevertheless, a reduction in the load admittance at any node enables the possibility of obtaining the convergence by increasing the admittance at some other node. Thus Eq. (13) provides only a sufficient condition for convergence. An alternative formulation which takes into account the infinite norm is given in the Appendix A.

4.3. Characteristics of the iterative process

Let us consider the iterative process (7). If all the elements of the matrix $\mathbf{B}$ do not depend on k (constant admittance loads) and $\mathbf{v}^{(0)} = V_0 \mathbf{l}$, then the voltage variation at the first iteration is $\Delta\mathbf{v}^{(1)} = \mathbf{B}\mathbf{v}^{(0)}$ and the voltage variation at the iteration k is related to the one at the iteration $(k-1)$ by the expression

$$\Delta\mathbf{v}^{(k)} = \mathbf{B}\Delta\mathbf{v}^{(k-1)} = \mathbf{B}^k \mathbf{v}^{(0)} \tag{14}$$

According to the definition of the infinite norm (see Appendix A), after the first iteration the maximum variation of the complex voltage is

$$\|\Delta\mathbf{v}^{(1)}\|_\infty = V_0 \|\mathbf{B}\|\infty \tag{15}$$

and after the kth iteration it becomes

$$\|\Delta\mathbf{v}^{(k)}\|_\infty = \|\mathbf{B}\Delta\mathbf{v}^{(k-1)}\|_\infty \le \|\mathbf{B}\|_\infty \|\Delta\mathbf{v}^{(k-1)}\|_\infty \le \|\mathbf{B}\|_\infty^k V_0$$
$$= \left(\|\Delta\mathbf{v}^{(1)}\|_\infty\right)^k / V_0^{k-1} \tag{16}$$

The convergence of the iterative process is reached when

$$\|\Delta\mathbf{v}^{(k)}\|_\infty < \Delta V_{\mathrm{MAX}} \tag{17}$$

It is possible to compute the estimate $\hat{K}$ of the number of iterations required for the convergence of the iterative process with all constant admittance loads. Using Eq. (17) with $k = \hat{K}$ and assuming $\Delta V_{\mathrm{MAX}} = 10^{-m}$ p.u. yields

$$\hat{K} > \frac{-m - \log_{10} V_0}{\log_{10}\|\Delta\mathbf{v}^{(1)}\|_\infty - \log_{10} V_0} \tag{18}$$

The above result is quite significant for the analysis of distribution systems. The norm $\|\Delta\mathbf{v}^{(1)}\|_\infty$ has the relevant meaning of maximum variation of the complex voltage after the first iteration. In typical distribution systems, where the angle difference among the node voltages is very small, $\|\Delta\mathbf{v}^{(1)}\|_\infty$ becomes similar to the maximum voltage drop obtained by using the shunt currents computed with the voltage V_0 in each node. For a reasonable value of V_0, it is possible to estimate the number of iterations required for the convergence of the iterative process on the basis of only two components, that is, the voltage tolerance and the maximum variation in the complex voltage at the first iteration. As an example, with $V_0 = 1$ p.u. and $\|\Delta\mathbf{v}^{(1)}\|_\infty = 0.1$ p.u. (a large value), the iterative process will converge after m iterations independently of the size of the distribution system. The estimate may be inaccurate if V_0 is far from the rated voltage.

4.4. Effects of the load representation

Let us consider a voltage-dependent load representation with complex power

$$\underline{S}(V) = P(V) + \mathrm{j}Q(V) = P_{\mathrm{REF}}\left(\frac{V}{V_{\mathrm{REF}}}\right)^\alpha + \mathrm{j}Q_{\mathrm{REF}}\left(\frac{V}{V_{\mathrm{REF}}}\right)^\beta \tag{19}$$

where $\underline{S}_{\mathrm{REF}} = P_{\mathrm{REF}} + \mathrm{j}Q_{\mathrm{REF}}$ is the complex power at the voltage V_{REF}. Typical cases are the constant power ($\alpha = \beta = 0$), constant current ($\alpha = \beta = 1$), and constant admittance ($\alpha = \beta = 2$), loads.

As previously shown, if all the loads have a constant admittance model the assessment of the sufficient condition for the convergence of the iterative process is straightforward. In the presence of any non-constant-admittance load in the network, the equivalent load admittance varies during

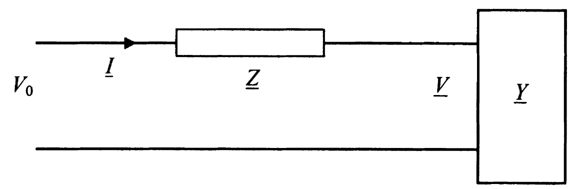

Fig. 2. Two-node system.

the iterative process. The assessment of the convergence conditions depends on the definition of the reference point in Eq. (19). The comparison may be set up in different ways. Let us consider two different frameworks:

Framework #1: The loads have different models and share the same power at the nominal voltage of 1 p.u. At the generic ith load node, the constant admittance load is defined using a per-unit admittance $\underline{Y}_i^{(0)} = \underline{S}_i$. This approach has been followed by Haque [14] and results in different solution points.

Framework #2: The loads have different models, defined to represent the same solution point ($\underline{S}_i$,V_i). The constant admittance load at the ith load node is defined using the per-unit admittance $\underline{Y}_i^{(\infty)} = \underline{S}_i/V_i^2$.

The analysis of the convergence conditions and of the voltage variation during the iterative process is performed in the following sections, with numerical examples referred to different types of voltage-dependent loads. In particular, the two "extreme" cases of constant power ($\alpha = \beta = 0$) and constant admittance ($\alpha = \beta = 2$) loads have been considered.

5. Two-node system

5.1. Convergence conditions

This analysis shows the effects of various types of load representations on the convergence of the iterative process for a simple two-node system (Fig. 2). The framework #2 is adopted here.

Assuming the initial condition $\underline{V}^{(0)} = V_0$, let $\underline{V}^{(0)}, \underline{V}^{(1)}, \ldots, \underline{V}^{(k)}, \ldots$ be the succession of the voltages at the load node, which converges at the solution $\underline{V}$. At the kth iteration:

$$\underline{V}^{(k)} = -\underline{Z}\underline{Y}^{(k-1)}\underline{V}^{(k-1)} + V_0 \tag{20}$$

Comparing Eq. (20) with Eq. (8), the matrix **B** is reduced to the scalar term $B^{(k)} = -\underline{Z}\underline{Y}^{(k)}$. The voltage error computed with respect to the solution $\underline{V}$ at the kth iteration is $\epsilon^{(k)} = \underline{V}^{(k)} - \underline{V}$. Considering two successive iterations, it is possible to write

$$\underline{\epsilon}^{(k+1)} = -\underline{Z}\underline{Y}^{(k)}\underline{\epsilon}^{(k)} + \underline{Z}(\underline{Y}^{(\infty)} - \underline{Y}^{(k)})\underline{V} \tag{21}$$

With constant load admittance $\underline{Y}$, the sufficient condition for

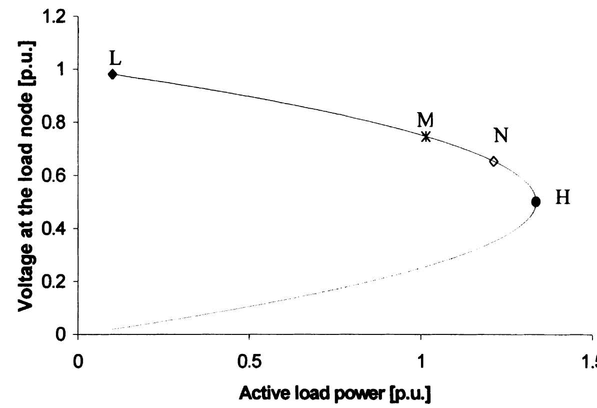

Fig. 3. $V(P)$ "nose" curve for the two-node system.

the convergence of the iterative process becomes

$$ZY < 1 \tag{22}$$

The limit condition $ZY = 1$ is the well-known condition of maximum power delivered to a load with given power factor. This maximum power is reached at the tip of the $V(P)$ "nose" curve which represents the network characteristic (Fig. 3). Thus the convergence of the iterative method is assured in the whole range of the feasible powers delivered to the load but the maximum power. The iterative process exhibits a first-order convergence, being for two successive iterations

$$\frac{\|\epsilon^{(k+1)}\|}{\|\epsilon^{(k)}\|} = ZY \tag{23}$$

For a generic voltage-dependent load, the equivalent admittance varies during the iterations. The convergence condition becomes

$$ZY^{(\infty)} < 1 \tag{24}$$

where the limit condition $ZY^{(\infty)} = 1$ again corresponds to the maximum power delivered to a load with given power factor. If the modulus Z of the line impedance and the power factor of the load are known, the maximum power does not depend on the type of load model (constant admittance, constant power, etc.). Thus, the convergence of the iterative method is assured for any load power up to the maximum power, independently of the load modelling. Furthermore, it is not possible to converge to a solution point located on the lower branch of the $V(P)$ curve, since all the points on the lower branch have an equivalent admittance higher than $Y^{(\infty)}$ and the condition (24) is not satisfied. This result is of utmost importance when multiple solution points do exist, as in the case of a constant power load. In this case, the performance of the backward/forward sweep method differs with respect to other load-flow algorithms (e.g. Newton–Raphson) which can also find the solutions on the lower branch of the $V(P)$ curve. Several tests confirmed that the iterative process converges at the solution located on the

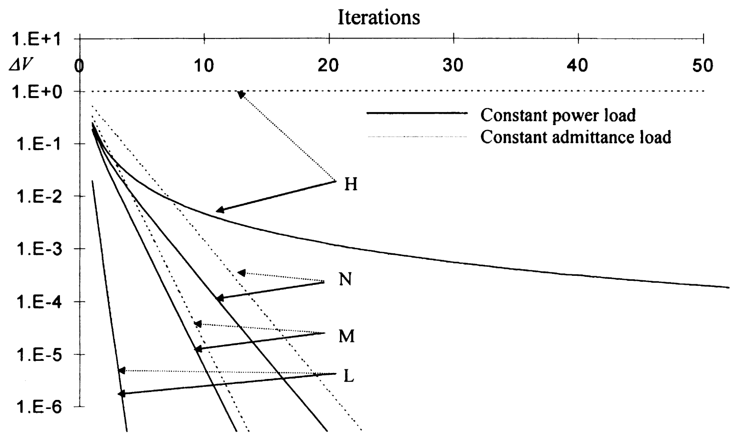

Fig. 4. Iterative process for the two-node system at different load levels.

upper branch of the $V(P)$ curve even using very different initial voltages at the load node, including very low voltages.

5.2. Analysis of the voltage variation during the iterative process

Assuming the initial voltage $V^{(0)}$ at the load node, the voltage variation at the kth iteration is

$$\Delta V^{(k)} = V^{(k)} - V^{(k-1)} \tag{25}$$

The iterative process terminates when the voltage variation becomes lower than the specified tolerance ΔV_{MAX}.

It is interesting to study how the convergence is reached for different load models. Let us adopt the framework #2. For any single point of the $V(P)$ curve, it is possible to build any type of load model which satisfies the local solution. The two-node system of Fig. 2 is used with $R = 0.15$ p.u., $X = 0.06$ p.u., $V_0 = 1$ p.u. and the base case load $P_L + jQ_L = 0.1 + j0.06$ p.u. (the point L in Fig. 4). In order to analyse the iterative process at different load levels, Let us start from the point L and let us consider a load increase path with constant ratio $Q/P = 0.6$. This path is represented by the $V(P)$ curve of Fig. 3 and terminates at the maximum loadability point H, in which $P_H + jQ_H = 1.33456 + j0.801274$ p.u. [15]. Let us consider four sample points on the $V(P)$ curve at different loading levels, namely, L, M, N and H. Table 1 shows the data of the sample points, being $P + jQ$ the complex load power referred to the constant power load, and V the receiving end voltage magnitude in the solution point, computed analytically by solving the bi-quadratic system equation

$$V^4 - 2\left(\frac{V_0^2}{2} - RP - XQ\right)V^2 + Z^2(P^2 + Q^2) = 0 \tag{26}$$

Table 1
Sample points

Point	P (p.u.)	Q (p.u.)	V (p.u.)
L	0.1	0.06	0.9810
M	1.0	0.60	0.7518
N	1.2	0.72	0.6607
H	1.335456	0.801274	0.5016

Starting from the initial voltage $\underline{V}^{(0)} = 1 + j0$ p.u., the iterative process is shown in Fig. 4 for different load representations and load levels. The constant admittance load is taken as a benchmark for assessing the evolution of the iterative process.

5.3. Constant admittance load

Starting from $V^{(0)} = V_0$ at the receiving node, the voltage variation at the first iteration is

$$\Delta V^{(1)} = -ZYV_0 \tag{27}$$

Assuming the voltage variation tolerance $\Delta V_{MAX} = 10^{-m}$, the convergence is reached after a number of iterations $\hat{K}$ computed analytically from Eq. (18), where the inequality turns to an equality due to the presence of all scalar terms:

$$\hat{K} = \frac{-m - \log_{10} V_0}{\log_{10} \Delta V^{(1)} - \log_{10} V_0} \tag{28}$$

5.4. General load modelling

Let us consider the voltage-dependent load representation (19), where $\alpha = \beta$, and $0 \le \alpha \le 2$. The interpretation of the iterative process depends on the framework assumed.

Framework #1: The voltage reference in Eq. (19) is the nominal voltage V_0. The equivalent admittance has the same initial value $\underline{Y}^{(0)}$ for all the load models and vary at any iteration k during the iterative process. The relation $\underline{Y}^{(0)} \le \underline{Y}^{(k)} \le \underline{Y}^{(\infty)}$ holds, but the final value $\underline{Y}^{(\infty)}$ depends on α. The constant admittance load model has the lowest value of $\underline{Y}^{(\infty)}$. The solution point, if it does not exceed the loading limits, is closer to the tip of the $V(P)$ curve for lower values of α. By this way, the iterative process

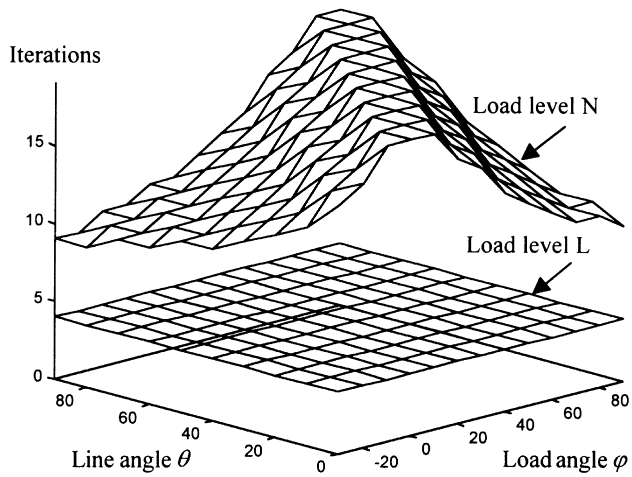

Fig. 5. Effect of different load and line impedance angles.

exhibits a better convergence if the solution point remains far from the loading limit, that is, using the constant admittance load model.

Framework #2: The reference point in Eq. (19) is the solution point located on the $V(P)$ curve, with voltage magnitude V. The apparent power is $S = g(\alpha)V^{\alpha}$ and the magnitude of the equivalent admittance at the kth iteration is

$$Y^{(k)} = \frac{S}{(V^{(k)})^2} = \frac{g(\alpha)}{(V^{(k)})^{2-\alpha}} \tag{29}$$

Starting from a voltage $V^{(0)} > V$, then $\underline{Y}^{(0)} \leq \underline{Y}^{(k)} \leq \underline{Y}^{(\infty)}$ for any iteration k during the iterative process. If the load admittance were constant at any value lower than $Y^{(\infty)}$, the iterative process would be faster than the one with constant admittance $Y^{(\infty)}$. Then, considering the whole iterative process, a faster convergence is obtained in the presence of any voltage-dependent load with $0 \leq \alpha < 2$, with respect to a constant admittance load corresponding to the same solution.

Particularly interesting from a computational viewpoint is the iterative process in the load limit case where the solution point lies on the tip of the $V(P)$ curve. Let us fix a voltage variation tolerance ΔV_{MAX}. Using a constant admittance load, the lack of convergence is immediately detected ($\Delta V^{(k)} = 1$ for any kth iteration), while for any case with $0 \leq \alpha < 2$ the constant voltage variation (horizontal slope) is reached only asymptotically, making it possible to detect a convergence in a very large number of iterations. Fig. 4 shows this behaviour using a constant power load, where this effect is quite evident at high load levels.

Table 2
Iterative process with constant admittance and constant power loads

		Framework #1			Framework #2		
Load factor F	K_S	$\|\Delta\mathbf{v}^{(1)}\|_\infty$	$\hat{K}_{Y0}$	K_{Y0}	$\|\Delta\mathbf{v}^{(1)}\|_\infty$	$[\hat{K}]$	$[K_Y]$
1	6	0.1165	5.4	5	0.1461	6.0	6
2	10	0.2330	7.9	8	0.4248	13.4	11
2.5	22	0.2912	9.3	9	0.8200	58.0	29
2.6	104	0.3029	9.6	9	1.1885	<0	253
2.60128	235	0.3030	9.6	9	–	–	∞

5.5. Effect of the line and load angles

The number of iterations necessary to reach the convergence for the two-node test system under a voltage variation tolerance $\Delta V_{\mathrm{MAX}} = 10^{-6}$ is plotted in Fig. 5 for different load angles $\varphi = \arctan(Q/P)$ and line impedance angles $\theta = \arctan(X/R)$. A constant power load model is used at different load levels. At each load level, the values of P and Q are chosen for different load angles φ by maintaining the same apparent power. In the same way, the line parameters R and X for different angles θ are defined by maintaining the magnitude of the line impedance Z constant. Fig. 5 shows the results using two load levels corresponding to the points L and N of Fig. 3. At the lower load level L, the number of iterations is constant. When the load level increases, the number of iterations depends on the angles φ and θ, while the typical dependencies of other computational methods, as the X/R ratio [8] or the nature of the load, are not relevant in this case. For each load angle, the number of iterations is the highest in the case $\varphi = \theta$, which corresponds to a voltage drop in phase with the voltage at the load terminals and leads to the lowest voltage at the load terminals in the solution point.

6. 84-node system

An example is presented using an 84-node rural distribution system [5]. Starting from the base case, the loads are increased uniformly. The scalar load factor F is used to represent the load variation. The load factor corresponding to the point located on the critical boundary, computed with a dedicated method [16], is $F^{\max} = 2.60128$. Let us assume the root node voltage $V_0 = 1$ p.u. and all the load node voltages starting from $\mathbf{v}^{(0)} = V_0\mathbf{l}$. The results are presented in Table 2 for different loading levels using the two frameworks. With constant power loads, the iterative process converges in K_S iterations for each load factor.

To estimate the number of iterations required to reach the convergence, the authors propose to monitor the ratio between the maximum voltage variation for each pair of successive iterations, defined as:

$$\chi^{(k)} = \|\Delta\mathbf{v}^{(k)}\|_\infty / \|\Delta\mathbf{v}^{(k-1)}\|_\infty \tag{30}$$

6.1. Framework #1

With constant admittance loads, the norm $\|\Delta\mathbf{v}^{(1)}\|_\infty$ computed at the first iteration is used to compute the estimate $\hat{K}_{Y0}$ of the number of iterations K_{Y0} using Eq. (18), resulting in a quite accurate approximation. The indicator

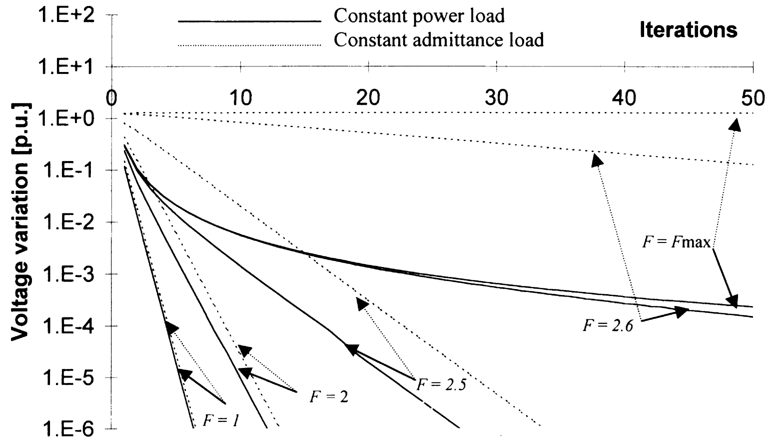

Fig. 6. Voltage variation with constant power and constant admittance loads for different loading levels.

$\chi^{(k)}$ is nearly constant during the iterative process, with slight variations due to the inequalities in Eq. (16).

6.2. Framework #2

The iterative process (Fig. 6) exhibits the same behaviour as for the two node system, and it is possible to detect a convergence with constant power loads even in the maximum power conditions (load factor $F^{\max}$) using a strict tolerance (e.g. $\Delta V_{\mathrm{MAX}} = 10^{-5}$ p.u.).

If all the loads have constant admittance, it is possible to use Eq. (18) to estimate in how many iterations the iterative process will converge with voltage tolerance ΔV_{MAX} after performing only the first iteration. Table 2 shows the results for $\Delta V_{\mathrm{MAX}} = 10^{-5}$ p.u. and different load factors. Note that in this case the application of Eq. (18) using the norm $\|\Delta \mathbf{v}^{(1)}\|_\infty$ does not give always accurate results, $\hat{K}$ being largely overestimated with respect to the actual value K_{Y} at high load factors and resulting in unfeasible values when the solution point is close to the load limit (but the iterative process converges).

Table 2 also shows that K_{S} is always lower than K_{Y}, confirming that the same solution point is reached in a faster way with constant power rather than with constant admittance loads.

With constant admittance loads, $\chi^{(k)}$ has a slight variation during the iterative process (Fig. 6), tending to the asymptotic value $\chi^{(\infty)}$ which is the same asymptotic value reached with constant power loads, provided that the loads are defined to represent the same solution.

At each iteration, the estimate $\hat{K}_{\mathrm{Y}}^{(k)}$ of the number of iterations required to reach the convergence has been computed using $\chi^{(k)}$ instead of the norm $\|\Delta \mathbf{v}^{(1)}\|_\infty$ in Eq. (18). Fig. 7 shows the evolution of $\hat{K}_{\mathrm{Y}}^{(k)}$ during the iterative process. It is worthwhile to note that a good estimate of the actual number of iterations K_{Y} is already achieved after a few iterations, even in the case of very high load factors, in spite of the fact that the evolution of $\chi^{(k)}$ may follow unpredictable trends in the initial iterations, with possible low oscillations as observed during several tests. The values $\chi^{(k_{\mathrm{Y}})}$ and $\hat{K}_{\mathrm{Y}}^{(k_{\mathrm{Y}})}$ shown in Table 3 are the approximations of $\chi^{(\infty)}$ and $\hat{K}_{\mathrm{Y}}^{(\infty)}$ computed at the last iteration K_{Y}.

Assuming the common initial values for the iterative process, with all the voltages starting from V_0, the

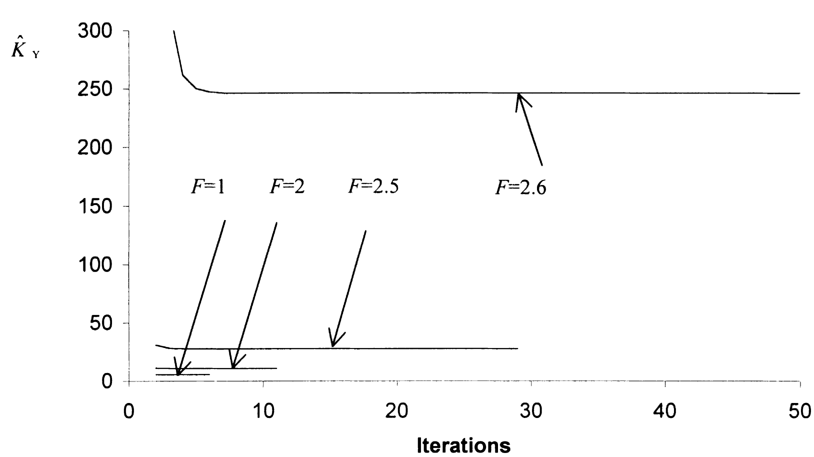

Fig. 7. Estimate of the number of iterations required to converge.

Table 3
Estimate of the number of iterations for convergence (Framework #2)

Load factor F	$\chi^{(k_Y)}$	$\hat{K}_Y^{(k_Y)}$	K_Y
1	0.1178	5.4	6
2	0.3423	10.7	11
2.5	0.6592	27.6	29
2.6	0.9543	246.1	253
2.60128	1.0000	∞	∞

equivalent admittance of each non-constant admittance load gradually increases during the iterative process, tending to the final value $Y^{(\infty)}$. Correspondingly, the indicator $\hat{K}_Y^{(k)}$ rapidly approaches its asymptotic value $\hat{K}_Y^{(\infty)}$. Is then possible to get a satisfactory estimate of the number of iterations required to reach the convergence for a given voltage tolerance by monitoring $\hat{K}_Y^{(k)}$ during the iterative process.

7. Conclusions

A study on the convergence of the backward/forward sweep method for the solution of radial distribution networks has been presented. The behaviour of the method has been investigated in detail for different load models. Adopting the constant admittance load model, the iterative process converges for all the feasible operating conditions but the one of maximum power delivered to the loads. The convergence depends on the magnitude of the equivalent line impedance and load admittance, and it is not primarily affected by the load power factor and by the line X/R ratio.

In the presence of different voltage-dependent loads, the interpretation of the iterative process depends on the framework adopted for the analysis. From a system viewpoint, in which the different types of loads assumed correspond to the same solution point, a better convergence is reached with constant power loads rather than with constant admittance loads corresponding to the same solution. This result is different with respect to other traditional methods for the load-flow computation, as Gauss–Seidel or Newton–Raphson. The result is opposite if the voltage-dependent loads are defined in such a way to share the same power at the nominal voltage.

The evolution of the iterative process has been analysed at different load levels, showing the differences for various load models at high load level, up to the theoretical loadability limit of the system. In the normal operation of the distribution network, the load level is typically low and very distant from this limit, and the backward/forward sweep method generally exhibits a fast and reliable convergence for any load model and with different initial conditions.

Finally, simple relations have been given to estimate the number of iterations required for the convergence of the iterative process. A first relation is based on the maximum voltage variation at the first iteration and on the voltage tolerance required. It gives acceptable results for constant admittance loads at low and medium load levels, and it may also be useful with any type of load model at a low load level. For higher load levels and different load models, it is possible to obtain a refined estimate by monitoring the ratio between the maximum voltage variation for each pair of successive iterations during the iterative process.

Appendix A

Let us consider the iterative process

$$\mathbf{x}^{(k)} = \mathbf{B}\mathbf{x}^{(k-1)} + \mathbf{c} \tag{A1}$$

where the elements of the matrix $\mathbf{B}$ and of the vector $\mathbf{c}$ are independent of $\mathbf{x}$. Let us define $\rho(\mathbf{B})$ as the maximum absolute eigenvalue of the matrix $\mathbf{B}$. It is known from the numerical analysis [17] that the iterative process converges if and only if $\rho(\mathbf{B}) < 1$.

Furthermore, considering any norm $\|\mathbf{B}\|$ of the matrix $\mathbf{B}$ consistent with a vector norm, then $\rho(\mathbf{B}) \le \|\mathbf{B}\|$ and a sufficient condition for convergence is

$$\|\mathbf{B}\| < 1 \tag{A2}$$

Let γ_{ij} be the generic coefficient of the matrix $\mathbf{\Gamma}$ and Z_{Bii} and Y_{Sii} be the magnitudes of the diagonal terms of the matrices $\mathbf{Z}_B$ and $\mathbf{Y}_S$, respectively. Let us rewrite Eq. (A2) using two different norms:

1. the unity norm $\|\mathbf{B}\|_1$, which is the maximum of the sum of the absolute values of the elements in each column of the matrix $\mathbf{B}$, leading to

$$\max_{j=1,\dots,n} (\zeta_j) < 1 \tag{A3}$$

where

$$\zeta_j = \sum_{i=1}^{n} |b_{ij}| = Y_{Sjj} \sum_{k=1}^{j} \left| \gamma_{jk} Z_{Bkk} \sum_{i=k}^{n} \gamma_{ik} \right| = Y_{Sjj} Z_{Uj} \tag{A4}$$

2. the infinite norm $\|\mathbf{B}\|_\infty$, which is the maximum of the sum of the absolute values of the elements in each row of the matrix $\mathbf{B}$, leading to

$$\max_{i=1,\dots,n} (\xi_i) < 1 \tag{A5}$$

where

$$\xi_i = \sum_{k=1}^{n} |b_{ik}| = \sum_{k=1}^{n} Y_{Skk} \left| \sum_{j=1}^{k} Z_{Bjj} \gamma_{ij} \gamma_{kj} \right| \tag{A6}$$

The latter formulation takes into account the simultaneous presence of the loads located in the nodes along the path from the root to the ith node. The extreme case corresponds to a network with a unique load at the ith node, fed from lines having only series parameters along the path from the ith node to the root, and being Z_i^{TOT} the magnitude of the sum of the series line impedances. The two-node equations apply in this case, obtaining for the ith node a maximum admittance $Y_i^{\mathrm{MAX}} = 1/Z_i^{\mathrm{TOT}}$.

References

[1] Goswami SK, Basu SK. Direct solution of distribution systems. IEE Proceedings—C 1991;138(1):78–88.
[2] Cheng CS, Shirmohammadi D. A three-phase power flow method for real-time distribution system analysis. IEEE Transactions on Power Systems 1995;10(2):671–9.
[3] Thukaram D, Wijekoon Banda HM, Jerome J. A robust three phase power flow algorithm for radial distribution systems. EPSR 1999;50:227–36.
[4] Renato Cespedes G. New method for the analysis of distribution networks. IEEE Transactions on Power Delivery 1990;5(1):391–6.
[5] Das D, Kothari DP, Kalam A. Simple and efficient method for load flow solution of radial distribution networks. EPES 1995;17(5):335–46.
[6] Baran ME, Wu FF. Optimal sizing of capacitors placed on a radial distribution system. IEEE Transactions on Power Delivery 1989;4(1):735–43.
[7] Zhang F, Cheng CS. A modified Newton method for radial distribution system power flow analysis. IEEE Transactions on Power Systems 1997;12(1):389–97.
[8] Wu FF. Theoretical study of the convergence of the fast decoupled load flow. IEEE Transactions on PAS-96 1977;1:268–75.
[9] Luo GX, Semlyen A. Efficient load-flow for large weakly meshed networks. IEEE Transactions on Power Systems 1990;5(4):1309–16.
[10] Rajicic D, Taleski R. Two novel methods for radial and weakly meshed network analysis. EPSR 1998;48:79–87.
[11] Lin CE, Huang YW, Huang CL. Distribution system load-flow calculation with microcomputer implementation. EPSR 1987;13:139–45.
[12] Shirmohammadi D, Hong HW, Semlyen A, Luo GX. A compensation-based power flow method for weakly meshed distribution and transmission networks. IEEE Transactions on Power Systems 1988;3(2):753–62.
[13] Broadwater RP, Chandrasekaran A, Huddleston CT, Khan AH. Power flow analysis of unbalanced multiphase radial distribution system. EPSR 1988;14:23–33.
[14] Haque MH. Load flow solution of distribution systems with voltage dependent load models. EPSR 1996;36:151–6.
[15] Bompard E, Carpaneto E, Chicco G, Napoli R. Evaluation of the critical load increase direction in voltage collapse studies. Electric Power Systems Research 1997;43(1):61–7.
[16] Carpaneto E, Chicco G, Napoli R, Piglione F. A Newton–Raphson method for steady-state voltage stability assessment. International Workshop Bulk Power System Voltage Phenomena II—Voltage Stability and Security. Deep Creek Lake, McHenry, Maryland, 4–7 August 1991. p. 341–5.
[17] Ralston A, Rabinowitz P. A first course in numerical analysis. 2nd ed. 1978 (International Student Edition, McGraw Hill, Auckland).